Electrochemical Atomic Force Microscopy of Electroactive Surfaces

1. Abstract

With the current requirement to reduce carbon dioxide emissions globally there is growing interest in trying to reduce the molecule to more relevant hydrocarbons, with the use of transition metal electro-catalysts. Direct reduction to usable compounds such as methanol is a possibility but slow reaction rates need to be improved. The anchoring of transition metal catalysts to light harvesting semiconducting surfaces offer the ability to increase reaction rates. The orientation of the catalysts when attached is a key issue as sterically carbon dioxide must be able to attach to the transition metal centre. It is for this reason that the surface chemistry is of vast importance. EC-AFM is a powerful tool that can be used for surface imaging as electrochemical reactions are taking place. Standard AFM can be used to image a layer of TiO_2 deposited on elemental titanium. It is possible to get down to 0.5um before distortion with an unpolished surface. The growth of TiO_2 on the surface occurs in dome like clusters that are not uniform in their positioning.

2. Introduction

Atomic force microscopy, AFM is a microscopic technique, invented in 1986[1] that can be used to attain excellent resolution of surfaces giving an insight into surface morphology at the atomic scale. It has been utilised extensively with biological samples such as cells [2] and semiconducting surfaces [3]. The system incorporates a micro tip attached to a cantilever that moves up and down on its z-axis as it deflects off a samples surface [4]. The micro tip is extremely small and usually extends to a single atom. In a typical scan the tip is in contact with the surface and raster scanned over the area of interest in the x and y directions. As the tip moves across the material it can move up and down the z-axis as a function of the force between tip and sample. For imaging purposes the constant distance from the sample requires the use of constant force between the material and micro tip. This is achieved by a feedback loop. The loop consists of a laser, data processing unit, piezoelectric transducer and cantilever as shown in Figure 1. Movement of the cantilever changes the angle of incidence of the laser, which is recorded *via* the four quadrant photosensitive diode and relayed back from it to the data processing unit. The data processing unit can then control the sample position relative to the information processed with changes in voltage applied to the piezoelectric transducer. This maintains the constant force required between tip and sample in the z direction. There are three modes of use, contact, none contact and intermittent contact [5]. With contact mode the tip is in contact with the sample through the entire raster scan with the force kept constant as mentioned above. Intermittent and none contact are generated by oscillating the cantilever near or slightly above its resonance frequency [1]. None contact mode makes use of Van der Walls forces between the atoms of the surface and the micro tip. Contact mode is too harsh for some materials such as certain biological samples due to substrate deformations [6]. This is a result of too much force between sample and the tip [7]. None contact mode is one way around this, however this is at the expense of resolution. Intermittent or as it is sometimes called intermittent tapping mode is a compromise between these two techniques as the tip is in contact infrequently, cutting down on the excess force [8].

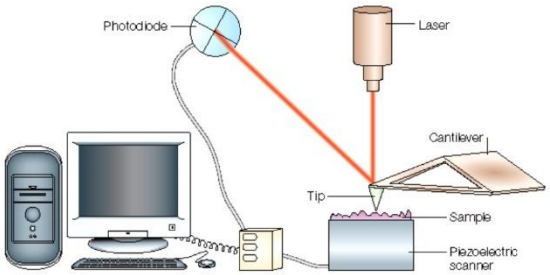

Figure 1. Schematic of an AFM system and its components [27]

AFM is analogous to the standard tunnelling microscope, however it does not require the tunnelling currents between tip and surface meaning that it can detect none conductive molecules [9]. Moreover it has now been established that it can be used for electrochemical surface imaging with the realisation of electrochemical AFM, EC-AFM. Over the last decade this new technique has developed into a powerful tool in particular in the study of lithium ion batteries and semiconducting materials. Figure 2 shows a standard EC-AFM setup with a gold working electrode. Here the probe works independently building up a topographical image of the surface as the electrochemical reaction proceeds. There is also another method where the tip is configured to act as the working electrode, ideal for the study of electrode kinetics [10]. Of particular interest is the semiconductor titanium dioxide (TiO_2). The knowledge of its surface properties are vital as it is used as an electrochemical catalyst, alloy film and medical implantation species. In 2001 EC-AFM was used to image the saline based oxide hydration of TiO_2 relevant to its electrochemical behaviour as a bio implant, in its freely corroding and potentiostatically held state (-1V), thus allowing simultaneous investigation of its surface morphology and electrochemical characteristics [11]. High resolution images of grain boundaries have be resolved as seen with titanium based alloys resulting in scan dimensions of $10\mu m^2$, where EC-AFM has provided insight into how the surface of an alloy changes in respect to the corrosion rates of each individual phase within the alloy [12]. To the knowledge of this paper examples of EC-AFM for analysis of TiO_2 are scarce with more emphasis given to its use in the study of lithium ion electrodes [13].

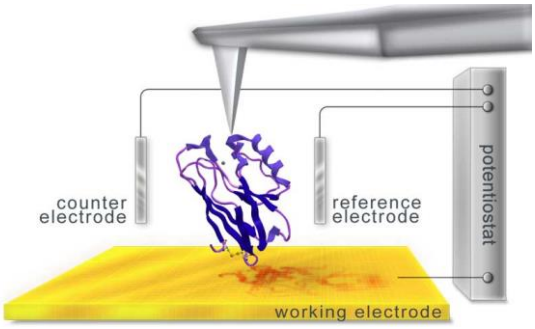

Figure 2. EC-AFM setup where the working electrode contains an anchored molecule [28]

With the current ambition of CO_2 removal from the atmosphere there is much interest in breaking down the molecule to more favourable C1 compounds [14]. Catalytic transition metal complexes can be used to reduce CO_2. These electro-catalysts rely on electron donation from the catalyst to the molecule. It is desirable to avoid single electron transfer in order to achieve thermodynamically stable species, *via* multi electron and proton reactions, as single electron donation results in $CO_2^{\cdot-}$ formation [15]. There are many transition metal complexes that can catalyse CO_2 reduction. Re and Ru based carbonyl complexes that contain bi-pyridine ligands have seen much attention due to high efficiencies [16]. These types of rare metals are too expensive for large scale use. The reduction of CO_2 needs to be more cost effective before scale up is achievable. Recently there has been research into using a Mn complexes for CO_2 reduction. *fac*-$Mn(bpy)(CO)_3Br$ has been shown to reduce the molecule however with relatively small turnover number of 13[17]. Using this same complex in a photocatalytic system utilising $[Ru(dmb)_3]^{2+}$ as a photosensitizer in DMF and TEOA a turnover number, TON of 149 was achieved for the reduction of CO_2 to formic acid[16]. The reduction rates of these complex catalysts do require selectivity towards CO_2 and one proposed way of increasing the reaction rate is to anchor the transition metal complex to a semiconductor such as TiO_2, that once exited with UV radiation has the ability to transfer electrons from its conduction band to the catalyst *via* an anchoring group such as a carboxylate or phosphonate. There are not many examples of electro catalysts being anchored for the above purpose, all but a few. Anchoring with carboxylate and phosphonate functional groups has been successfully demonstrated in the direct covalent bonding of a ruthenium sensitizer complex to a TiO_2 surface albeit the transfer of electrons was from the dye to the semiconductor [18]. The rates of reaction regarding CO_2 reduction have been compared between activity of a complex catalyst when anchored and unanchored to a semiconductor, where for the first time a nickel cylam catalyst was successfully anchored to a TiO_2 surface with the conclusion that the rate was improved upon attachment [19]. Rhenium complexes containing different ligands have been studied quite extensively through the years in order to achieve a catalyst that can selectively reduce CO_2, one example being $Re(dcbpy)(CO)_3Cl$ (dcbpy = 4,4'-dicarboxy-2,2'-bipyridine) that was shown to have higher reduction capability when anchored to

TiO_2[20]. Reduction with cobalt complex catalysts are another area of research. It was reported that [Co(cyclam)Cl_2]Cl attained a TON of 54 for CO after the reduction of CO_2 for one hour using *p*-terphenyl as a photosensitiser [21]. In 2014 this TON was increased to 55 and 64 when the catalyst was deposited, possibly uniformly on a TiO_2 surface made up of 80% anatase and 20% rutile [22]. The TiO_2 in this study was used as the photosensitizer donating electrons to the deposited catalyst upon photo-excitation. It is vital that the binding modes of these catalysts when anchored to semiconducting surfaces and their orientation when in place are fully understood to allow the fine tuning of their catalytic properties. The transition metal centres must be orientated at an ideal position to allow CO_2 coordination. In 2012 using phase-sensitive vibrational sum frequency generation spectroscopy the tilt angle of a rhenium bipyridyl CO_2 reduction catalyst on a single crystal of rutile TiO_2 was investigated when it contained different numbers of spacer methylene groups between the carboxyl anchor and the bipyridyl ligand [20]. The molecular tilt on the surface was shown to be a function of the number of methylene spacer groups, indicating a possible method of tailoring surface orientation.

Mentioned above, EC-AFM with its enhanced resolution and ability to image surfaces as electrochemical reactions proceed would allow a better understanding of how these catalysts pack onto the semiconducting surfaces, their orientation, key differences relating to synthetic routes and how surface morphology affects the rates of CO_2 reduction. In this paper a standard AFM experiment is set up and used to investigate the surface morphology of TiO_2 grown on elemental titanium metal and a complex catalyst, Re(dcbpy)$(CO)_3$Cl is synthesised for future use with EC-AFM when anchored to anatase TiO_2.

3. Method

Re(dcbpy)$(CO)_3$Cl was prepared by adding 0.5 mol of Re(CO_5)Cl and 0.5 mol of 4,4'-dicarboxy-2,2'-bipyridine to a beaker, then 20ml of toluene. This mixture was refluxed for three hours at 116C which gave a yellow liquid. It was then cooled to room temperature. 10 ml of hexane was added to the mixture once cooled to allow precipitation. The product was then washed with 3 ml toluene and dried in vacuo. The compound was then scanned using NMR (400MHz). Mass spec was also taken of the sample using time of flight.

TiO_2 was synthesised through heating a $4cm^2$ piece of pure titanium metal of approximately 1.5 mm thickness at 450C for 1 hour to attain a layer of anatase over the surface.

EC-AFM measurements were carried out on a Bruker Icon AFM machine using the scan assist mode. X-Y Scan range 90µm x 90µm x 10µm, Vertical noise floor <30 pm RMS, motorised position stage of X-Y axis 180 -150mm and a 210mm vacuum chuck.

4. Results and Discussion

The mass spectrum did show a main peak at 594.2m/z, corresponding to the molecular weight of Re(dcbpy)$(CO)_3$Cl, however other masses where abundant as the spectrum showed, Please see attached spectrum. From NMR analysis it was quite apparent that the desired molecule was not detected, observed in Figure 3. The main peak at 2.5ppm was a quintet. This was from the DMSO as the commercially available forms are not 100% pure [23]. Four other peaks were observed implying the facial structure due to molecular symmetry [24], however this was not the case as there would have been four separate proton environments. Integral ratios also discounted this as they should have been equal. The carboxylate functional groups should have appeared around 10-11ppm so this was another indicator of the signals not arising from the Re(dcbpy)$(CO)_3$Cl species. It was possible there was not enough of the compound dissolved into the DMSO and with the impure nature already mentioned no viable signal could be obtained.

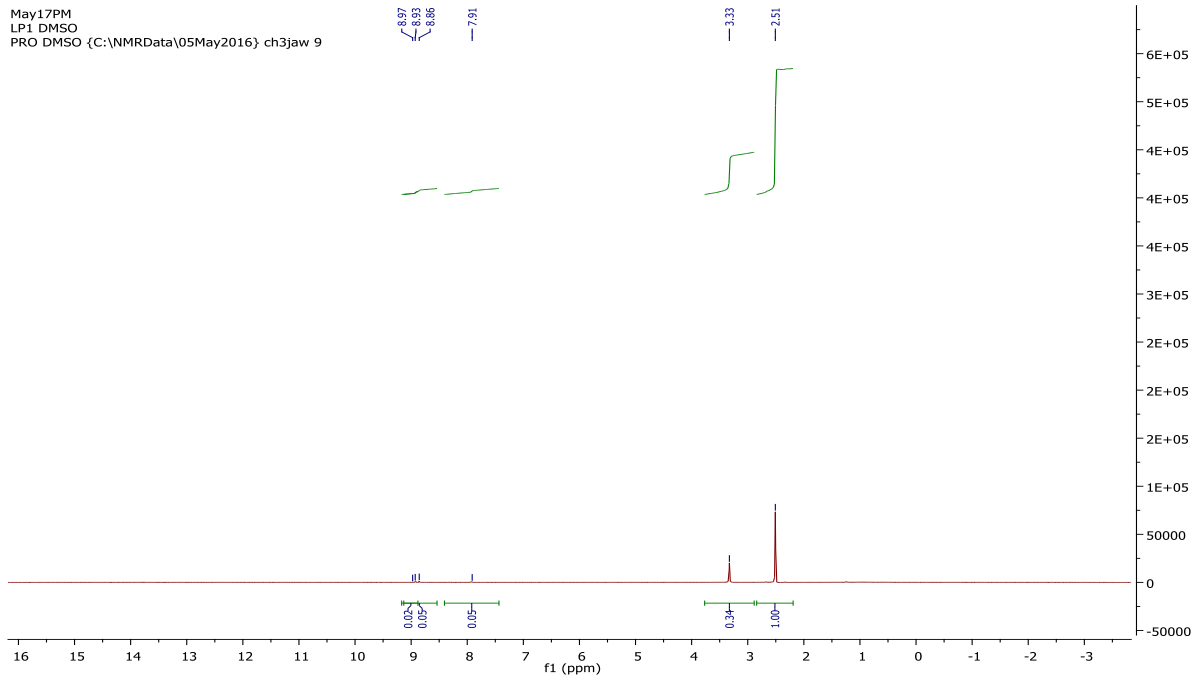

Figure 3. ^{1}H NMR signals of sample dissolved in DMSO

Imaging of the TiO_2 covered surface was achieved. Starting at 30 µm^2 and working down it was possible to get to 0.5 µm^2 with good resolution but going beyond this point to 0.4 µm^2 there was slight

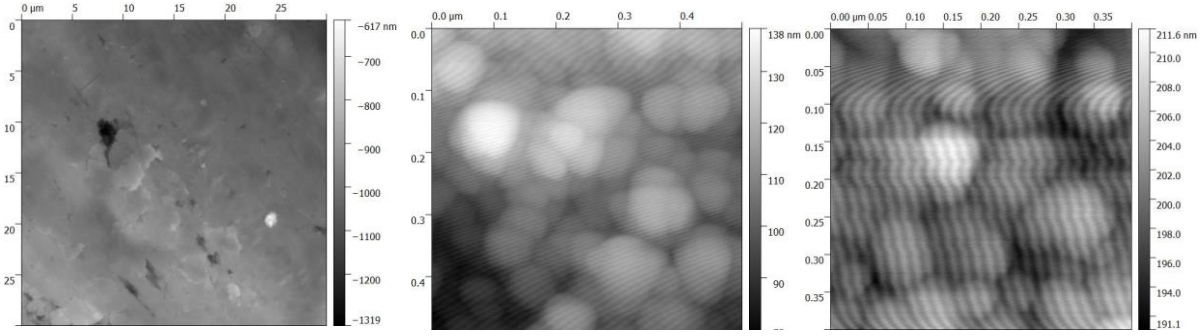

(a) (b) (c)

disturbance in the imaging as seen above with images (a), (b), and (c). Because of this no further images where taken as any closer recordings may have damaged the silicon stylus. The micro-tips used are so small with AFM the surface has to be very smooth as not to damage the tip as they are very sensitive. It has been mentioned elsewhere that TiO_2 is known to cover the surface in dome like clusters [25]. This was in keeping with the dome like structures imaged here in (b) and (c). Taking (b) and looking at the image in 3D (Fig. 4) the height of the highest point was 138nm and it was evident that the domes are not uniform on this surface as clusters occur at different heights and orientation. In (a) the black mark visible in the upper left quadrant was down to surface abnormalities believed to be caused by the preparation process of the TiO_2 layer. The surface was not polished and as such the zoom attainable was not as good as it perhaps could have been. It has been possible to attain much closer imaging with uniform surfaces. The lattice surface arrangement of mica substrates have been imaged at 0.036µm^2 [26].

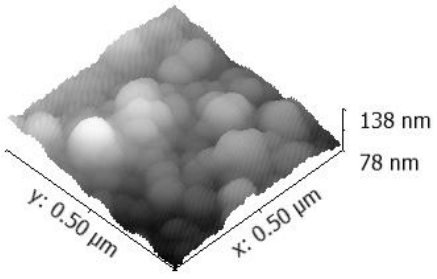

Figure 4. 3D image of (b)

Electro-polishing of the elemental titanium before the oxide layer was applied has been done before in AFM experiments [11]. This may have allowed a more even coverage of TiO_2 thus much closer imaging at clear resolution.

From the results, taking the synthesis and AFM imaging into account, it was quite evident that precise characterisation is required at each step from the synthesis of transition metal catalysts to the surfaces that they are to be attached. Each step is crucial before an EC-AFM experiment can be successfully run. Future work should include the setup of AFM in its EC-AFM mode and synthesis of molecules to be anchored. Infra-red spectroscopy will also be utilised to detect the stretch frequencies of the carbonyl groups of the complex catalyst. Adsorption spectroscopy could also be used. This will give another element to the successful characterisation of the materials. Standard AFM could still be used on the surface as was done in this study to investigate the oxide layer before attachment of the catalytic species. This can then be used to check the difference in catalytic orientation as a function of surface preparation. There are many considerations that have to be considered in the setup of an EC-AFM experiment such as how the cell is going to be constructed. One possible way would to be to bubble a certain concentration of CO_2 across the surface in a cell with a proton donor electrolyte, over a time frame and monitor the CO concentration at a specific reduction potential. This could be achieved using titanium as the working electrode, as the TiO_2 is already grown on it. Platinum would be used as a counter electrode with a standard AgCl reference electrode. With this in mind the system would have to be closed globally such as in a fume cupboard allowing inlet and outlet of the CO_2 through the electrochemical cell.

5. Conclusion

The compound $Re(dcbpy)(CO)_3Cl$ was created as shown in the mass spectrum but was not pure enough for use and as such never gave any clear proton NMR signals. It was possible to attain AFM images of TiO_2 grown on elemental titanium but the nature of the unpolished surface only allowed a zoom of $0.5um^2$ before the resolution started to degrade. The TiO_2 on the surface exists in dome like clusters, in agreement with other studies. The use of EC-AFM will be used in the future to characterise the surface of anchored electro-catalysts on semiconducting surfaces. Before this is done the electro catalysts and surfaces must be characterised efficiently.

References:

[1] Liu, S., & Wang, Y. (2010). Application of AFM in microbiology: A review. *Scanning*, *32*(2), 61-73.

[2] Li, M., Liu, L., Xi, N., Wang, Y., Dong, Z., Xiao, X., & Zhang, W. (2013). Progress of AFM single-cell and single-molecule morphology imaging. *Chinese Science Bulletin*, *58*(26), 3177-3182.

[3] Yoon, J., & Ivey, D. (1996). Preparation of cross-section specimens for AFM imaging of metal/semiconductor interfaces. *Journal of Materials Science Letters*, *15*(7), 551-554.

[4] *AFM Beginner's Guide*. (2009). *Afmhelp.com*. Retrieved 7 May 2016, from http://afmhelp.com/index.php?option=com_content&view=article&id=51&Itemid=57

[5] Skoog, D., Holler, F., & Crouch, S. *Principles of instrumental analysis* (p. 617).

[6] Persson, B. (1987). The atomic force microscope: Can it be used to study biological molecules? *Chemical Physics Letters*, *141*(4), 366-368.

[7] Casuso, I., & Scheuring, S. (2010). Automated setpoint adjustment for biological contact mode atomic force microscopy imaging. *Nanotechnology, 21*(3), 8.

[8] Vinckier, A., Hennau, F., Hellemans, L., & Kjoller, K. (1996). Low-cost modification of a contact atomic force microscope (AFM) into a sound-activated tapping mode AFM for use in air and liquids. *Review of Scientific Instruments, 67*(2), 387-392.

[9] Doi, Inaba, Tsuchiya, Jeong, Iriyama, Abe, & Ogumi. (2008). Electrochemical AFM study of LiMn $_2O_4$ thin film electrodes exposed to elevated temperatures. *Journal of Power Sources, 180*(1), 539-545.

[10] Macpherson, J. V., Unwin, P. R., Hillier, A. C., & Bard, A. J. (1996). In-situ imaging of ionic crystal dissolution using an integrated electrochemical/AFM probe. *Journal of the American Chemical Society, 118*(27), 6445-6452.

[11] Bearinger, Orme, & Gilbert. (2001). Direct observation of hydration of TiO_2 on Ti using electrochemical AFM: Freely corroding versus potentiostatically held. *Surface Science, 491*(3), 370-387.

[12] Chen, & Tsai. (2011). In situ corrosion monitoring of Ti–6Al–4V alloy in H 2SO 4/HCl mixed solution using electrochemical AFM. *Electrochimica Acta, 56*(4), 1746-1751.

[13] Wen, R., & Byon, H. (2014). In situ monitoring of the LiO_2 electrochemical reaction on nanoporous gold using electrochemical AFM. *Chemical Communications, 50*(20), 2628-2631.

[14] Kobayashi, K., Kikuchi, T., Kitagawa, S., & Tanaka, K. (2014). Selective Generation of Formamides through Photocatalytic CO_2 Reduction Catalyzed by Ruthenium Carbonyl Compounds. *Angewandte Chemie International Edition, 53*(44), 11813-11817.

[15] Benson, E. E., Kubiak, C. P., Sathrum, A. J., & Smieja, J. M. (2009). Electrocatalytic and homogeneous approaches to conversion of CO 2 to liquid fuels. *Chemical Society Reviews, 38*(1), 89-99.

[16] Takeda, H., Koizumi, H., Okamoto, K., & Ishitani, O. (2014). Photocatalytic CO_2 reduction using a Mn complex as a catalyst. *Chemical Communications, 50*(12), 1491-1493.

[17] Bourrez, M., Molton, F., Chardon-Noblat, S., & Deronzier, A. (2011). [Mn(bipyridyl)(CO) 3 Br]: An Abundant Metal Carbonyl Complex as Efficient Electrocatalyst for CO_2 Reduction. *Angewandte Chemie International Edition, 50*(42), 9903-9906.

[18] Bae, E., Choi, W., Park, J., Shin, H., Kim, S., & Lee, J. (2004). Effects of surface anchoring groups (Carboxylate vs phosphonate) in ruthenium-complex-sensitized TiO_2 on visible light reactivity in aqueous suspensions. *Journal Of Physical Chemistry B, 108*(37), 14093-14101.

[19] Neri, G., Walsh, J., Wilson, C., Reynal, A., Lim, J., Li, X., . . . Cowan, A. (2014). A functionalised nickel cyclam catalyst for CO_2 reduction: Electrocatalysis, semiconductor surface immobilisation and light-driven electron transfer. *Physical Chemistry Chemical Physics, 17*(3), 1562-1566.

[20] Anfuso, C. L., Ricks, A. M., Lian, T. F., Xiao, D. S., Negre, C., & Batista, V. (2012). Orientation of a series of CO_2 reduction catalysts on single crystal TiO_2 probed by phase-sensitive vibrational sum frequency generation spectroscopy (PS-VSFG). *Journal of Physical Chemistry C, 116*(45), 24107-24114.

[21] Matsuoka, S., Yamamoto, K., Pac, C., & Yanagida, S. (1991). Enhanced p-Terphenyl-Catalyzed Photoreduction of CO_2 to CO through the Mediation of Co(III)-Cyclam Complex. *Chem. Lett.*, (12), 2099-2100. http://dx.doi.org/10.1246/cl.1991.2099

[22] Jin, T., Liu, C., & Li, G. (2014). Photocatalytic CO_2 reduction using a molecular cobalt complex deposited on TiO_2 nanoparticles. *Chemical Communications, 50*(47), 6221-6224.

[23] Gottlieb, H. E., Kotlyar, V., & Nudelman, A. (1997). NMR chemical shifts of common laboratory solvents as trace impurities. *Journal of Organic Chemistry, 62*(21), 7512-7515.

[24] Sato, S., Morimoto, T., & Ishitani, O. (2007). Photochemical synthesis of mer-Re(bpy)$(CO)_3$Cl. *Inorganic Chemistry, 46*(22), 9051-3.

[25] Brown, G., Thundat, T., Allison, D., & Warmack, R. (1992). ELECTROCHEMICAL AND INSITU ATOMIC FORCE MICROSCOPY AND SCANNING TUNNELING MICROSCOPY INVESTIGATIONS OF TITANIUM IN OXALIC-ACID SOLUTION. *Journal Of Vacuum Science & Technology A-Vacuum Surfaces And Films, 10*(5), 3001-3006.

[26] Gupta, Hampton, Nguyen, & Miller. (2010). Crystal lattice imaging of the silica and alumina faces of kaolinite using atomic force microscopy. *Journal of Colloid And Interface Science, 352*(1), 75-80.

[27] *Microbial Nanowires | Geobacter.org*. (2016). *Geobacter.org*. Retrieved 9 June 2016, from http://www.geobacter.org/Nanowires

[28] *EC-AFM | Nolux Media*. (2016). *Noluxmedia.nl*. Retrieved 9 June 2016, from http://noluxmedia.nl/portfolio/ec-afm/